European Polymer Journal 131 (2020) 109706

Contents lists available at ScienceDirect

European Polymer Journal

journal homepage: www.elsevier.com/locate/europolj

Biobased high-performance tri-furan functional bis-benzoxazine resin derived from renewable guaiacol, furfural and furfurylamine

Rui Yang, Mengchao Han, Boran Hao, Kan Zhang*

Research School of Polymeric Materials, School of Materials Science and Engineering, Jiangsu University, Zhenjiang, Jiangsu 212013, PR China

ARTICLE INFO

Keywords:
Benzoxazine
Guaiacol
Furfural
Furfurylamine
High performance

ABSTRACT

A novel fully biobased tri-furan functional bis-benzoxazine resin has been synthesized using guaiacol, furfural, furfurylamine and paraformaldehyde as raw materials *via* a two-step reaction approach. The detailed chemical structure of this newly obtained bis-benzoxazine monomer has been identified by NMR and FT-IR spectroscopies and elemental analysis. In addition, another bio-based benzoxazine monomer has also been synthesized based on the Mannich condensation of guaiacol, furfurylamine and paraformaldehyde for comparison. The polymerization behaviors of benzoxazines are investigated by DSC and *in situ* FT-IR, and the thermal and fire-related performances of resulting thermosets are investigated by TGA and micro-scale combustion calorimetry (MCC), respectively. Notably, the corresponding polybenzoxazine derived from the newly developed tri-furan functional bis-benzoxazine shows very excellent thermal stability with a T_g of 290 °C and a T_{d10} (the temperature at a weight loss of 10%) of 375 °C in nitrogen atmosphere. Moreover, a non-ignitable polybenzoxazine has also been achieved as shown by the very low heat release capacity (30.4 J g^{-1} K^{-1}) and total heat release value (5.8 kJ/g), making this bio-based thermosetting resin a promising material for high-performance applications.

1. Introduction

Benzoxazine compounds have been well-known for a long time, extending many areas of investigation [1], for instance, antimicrobial system [2], optoelectronic materials [3], medicine [4], and precursors of thermosets [5]. Although the history for the last one, namely benzoxazine resins, is much shorter than other benzoxazine-related areas, it has been fast developed in recent years [6]. Various raw materials can be used for the synthesis of benzoxazines because of their extraordinary molecular-design flexibility. This unique molecular characteristic endows benzoxazine resins with many excellent properties, such as polymerization without adding any catalysts [7,8], outstanding thermal stability [9–12], high mechanical performance [13], good dielectric characteristics [14–17], and low surface free energy [17,18]. These advantages make benzoxazine resins attractive candidates for applying in the fields of electronic packaging, aerospace, composites, and coatings.

Meanwhile, benzoxazine resins are facing the problem of limited raw materials from petroleum resources as many other commercialized polymers. Nowadays the environmental problem has been brought into sharp focus due to the overuse of petroleum-based polymers [19]. Therefore, preparing bio-based polymeric materials from renewable resources is highly desired, which aims to satisfy the future sustainable development [20–22]. Bio-based materials are also desired in order to reduce our carbon footprint. Researchers have made great efforts on producing new generation of bio-based polymers, which are capable of competing with the traditional polymers based on petrochemistry [23,24]. Particularly, Anastas and Warner have reported a guidance, listing the relevance of using natural renewable raw materials [25]. In the past decade, efforts for developing polybenzoxazine thermosets by using bio-based benzoxazine resins have been widely investigated. Cardanol [26], resveratrol [27], vanillin [28], guaiacol [29], magnolol [30], coumarin [31,32], and eugenol [33] are most used examples of the phenolic sources to synthesize benzoxazine resins. In addition, stearylamine [29], furfurylamine [32–35] and dehydroabietylamine [36] have also been used extensively as amine sources in benzoxazine molecular designing.

Furfurylamine has been widely used as amine source for the benzoxazine designing, and it can be easily produced from furfural, which was listed as a top 10 value-added bio-based substance by the US Department of Energy [37]. The flexible methylene group between the furan ring and amine group may cause a certain mobility to the molecular chains during the cross-linking reaction. Besides, the high reactivity of furan ring from furfurylamine could contribute an additional cross-linked network compared with other amine derivatives, which generally results in high char yields of polybenzoxazines [38,39]. On

* Corresponding author.
E-mail address: zhangkan@ujs.edu.cn (K. Zhang).

https://doi.org/10.1016/j.eurpolymj.2020.109706
Received 9 March 2020; Received in revised form 16 April 2020; Accepted 17 April 2020
Available online 18 April 2020
0014-3057/

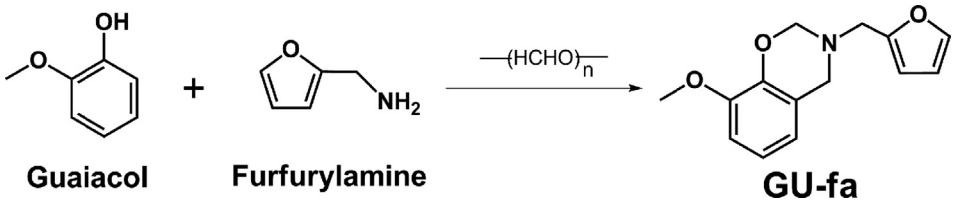

Scheme 1. Synthesis of the Guaiacol and Furfurylamine Based Mnono-Benzoxazine.

the other hand, guaiacol is a mono-phenolic compound that can be obtained through the pyrolysis of biomass. Previously, a fully biobased mono-functional benzoxazine derived from guaiacol and furfurylamine has been synthesized and investigated (Scheme 1) [29]. However, this benzoxazine monomer showed poor thermal stability during the polymerization, and its corresponding polybenzoxazine also exhibited very low T_g temperature (148 °C) [29]. Such results are not unexpected since mono-functional benzoxazines generally only lead to low molecular weight oligomers with large amounts of defect structures [11,40]. In addition, a bisguaiacol-F was synthesized and used to achieve bis-benzoxazine resins [41]. The polybenzoxazines derived from these bisguaiacol-F based bio-benzoxazines exhibited much higher thermal stability compared with traditional bisphenol-A based benzoxazine resin [41].

Inspired by the recently developed molecular design approach for improving the performance of guaiacol based mono-benzoxazines, we report a novel tri-furan functional bis-benzoxazine in this study. First of all, a bio-based bis-phenol containing furan ring was synthesized by a base-catalyzed condensation of natural renewable guaiacol and furfural in order to achieve tri-furan groups in one benzoxazine molecule. Then the bio-based tri-furan functional bis-benzoxazine was obtained using the above mentioned bio-based bis-phenol, furfurylamine and paraformaldehyde through a solventless method. Besides, the chemical structure of the newly developed bis-benzoxazine has been characterized using nuclear magnetic resonance (NMR) and Fourier infrared (FT-IR) spectroscopies, and elemental analysis. In addition, polymerization behaviors have been investigated by differential scanning calorimetry (DSC) and *in situ* FT-IR spectroscopy. Moreover, the thermal stability and flame-retardant properties of polybenzoxazines derived from both guaiacol-based mono- and bis-functional benzoxazines have also been studied and evaluated. Notably, the thermal and flame-retardant performances of the bio-based bis-benzoxazine resin have been found to be significantly higher than the guaiacol-furfurylamine based mono-functional benzoxazine resin. The molecular engineering strategy developed in the current study suggests the possibility of achieving high-performance thermosets using guaiacol, furfural and furfurylamine as renewable resources *via* benzoxazine chemistry.

2. Experimental

2.1. Materials

Guaiacol (99%), furfural (98%), paraformaldehyde (99%) and furfurylamine (98%) were obtained from Sigma-Aldrich. Hexane, toluene, ethyl acetate and sodium hydroxide (NaOH) were purchased from Aladdin Reagent, China and used as received. The guaiacol and furfurylamine based benzoxazine monomer, 3-(furan-2-ylmethyl)-8-methoxy-3, 4-dihydro-2*H*-benzo[e][1,3]oxazine (GU-fa), was synthesized according to the previously reported approach [29].

2.2. Characterization

^{1}H and ^{13}C NMR spectra were recorded on a NMR spectrometer (Bruker AVANCE, 400 MHz) at room temperature in deuterated dimethyl sufoxide using tetramethyl silane (TMS) as internal standard. Two dimensional NMR analysis of ^{1}H-^{1}H NOESY and ^{1}H-^{13}C HMQC were also performed on a Bruker AVANCE 400 spectrometer. FT-IR spectra were carried out at a resolution of 4 cm^{-1} on a spectrophotometer (Nicolet AVATAR-360). This spectrophotometer was equipped with a deuterated triglycine sulfate detector. The samples were grinded with potassium bromide (KBr) and pressed into KBr pellets for testing. Elemental analysis for the tri-furan functional bis-benzoxazine monomer was performed on the Elementar Vario EL-III analyzer. High resolution mass spectrometry (HRMS) was performed on a Bruker solanX 70 FT-MS mass spectrometer. A NETZSCH 204f1 instrument in nitrogen atmosphere was carried out at a heating rate of 10 °C/min to obtain differential scanning calorimetric (DSC) thermograms. Sealed aluminum oxide crucibles were used during the DSC measurements. The coefficient of thermal expansion (CET) was tested on a NETZSCH TMA/402F4 by thermomechanical analysis (TMA). A heating rate of 5 °C/min was performed during the TMA testing. Dynamic mechanical analysis (DMA) for polybenzoxazine was carried out by using a NETZSCH DMA/242E analyzer in air with an amplitude of 10 μm at a frequency of 1 Hz and a heating rate of 3 °C/min. The thermal stability of polybenzoxazines was determined by a TA thermal analyzer (Q50) in N_2 with a rate of 10 °C/min. Microscale combustion calorimeter (MCC, FAA-PCFC) was carried out to evaluate the flammability of polybenzoxazines [42]. A heating rate of 1 K/s and an 80 mL/min stream of nitrogen was applied for the measurement from 100 to 750 °C. In addition, the anaerobic pyrogenic decomposition products in N_2 stream were mixed with a 20 mL/min O_2 stream prior to sending it to the combustion furnace (the temperature was set as 900 °C).

2.3. Methods

2.3.1. Synthesis of 4,4′-(furan-2-ylmethylene)bis(2-methoxyphenol) (Abbreviated as FBP)

The approach to synthesize FBP was a modified method according to the procedure reported [43]. Guaiacol (5 g, 0.040 mol) and 20% aqueous NaOH (1.25 g) were mixed into a 100 mL two-necked flask equipped with an additional funnel. Furfural (2.01 g, 0.021 mol) was added slowly during the constant stirring. The reaction was kept for 6 h. Afterward the reaction was heated at 100 °C and kept stirring for 12 h. After reaction, the mixture was diluted by cold water and neutralized with hydrochloric acid. Then the precipitate was collected and dissolved in dichloromethane. The solution was washed by water for three times, and the organic layer was separated and dried by using anhydrous sodium sulfate. After removing the organic solvent by rotating evaporator, the product was purified by column chromatography using a hexane and ethyl acetate mixture (yield ca. 69%). ^{1}H NMR (400 MHz, DMSO-d_6), ppm: δ = 8.56 (d, 2H, −O*H*), 7.52 (d, 1H, −OC*H*═CH−), 6.85–6.38 (6H, Ar), 6.33 (m, 1H, CHR−C*H*═CHO), 6.08 (d, 1H, RC═C*H*−CHR), 5.72 (s, 1H), 3.78 (s, 6H, −C*H*$_3$). FT-IR spectra (KBr), cm^{-1}: FT-IR spectra (KBr), cm^{-1}: 3485 (−OH stretching), 1478 (C═C stretching of furyl ring), 1066 (C−O−C antisymmetric stretching), 828 (C−H wagging), 722 (out-of-plane of ═C−H).

2.3.2. Synthesis of 6,6′-(furan-2-ylmethylene)bis(3-(furan-2-ylmethyl)-8-methoxy-3,4-dihydro-2H-benzo[e][1,3]oxazine) (Abbreviated as FBP-fa)

A mixture of FBP (1.20 g, 0.0036 mol), furfurylamine (0.693 g, 0.0071 mol) and paraformaldehyde (0.481 g, 0.016 mol) was mixed into a 100 mL flask and stirred for 1 h. The reaction was then heated and stirred at 90 °C for 2 h. Afterward the solid sample was dissolved in chloroform, and washed three times with 1 N NaOH aqueous solution.

Then the solution was further purified by washing with distilled water for another three times. At last, the product was recrystallized from acetone to yield white crystals (yield ca. 76%). ^{1}H NMR (400 MHz, DMSO-d_6), ppm: δ = 7.60 (d, 3H, −OC*H*−CH), 6.67 (d, 2H, Ar), 6.43 (d, 2H, Ar), 6.39 (m, 3H, CHR−C*H*═CHO), 6.29 (d, 2H, RC═C*H*−CHR), 6.02 (d, 1H, RC═C*H*−CHR), 5.28 (s, 1H), 4.79 (s, 4H, Ar−O−CH_2−NR, oxazine), 3.87 (s, 4H, Ar−CH_2−NR, oxazine), 3.82 (s, 4H, RN−CH_2−fur), 3.68 (s, 6H, −CH_3). FT-IR spectra (KBr), cm^{-1}: 1496 (C═C stretching), 1227 (stretching vibrations of aromatic C−O linkages), 922 (oxazine ring related mode), 855 (C−H wagging), 734 (out-of-plane of ═C−H). Anal. Calcd. for $C_{33}H_{32}N_2O_7$: C, 69.70; H, 5.67; N, 4.93. Found: C, 69.62; H, 5.70; N, 4.89. HRMS-ESI (*m/z*): [M + H]$^+$ calculated for $C_{33}H_{33}N_2O_7^+$, 569.2282; found, 569.0572.

2.3.3. Polymerization of biobased benzoxazine monomers

The molten benzoxazine monomers, GU-fa and FBP-fa, were cast over a glass plate at 100 and 140 °C, respectively. The resulting films derived from GU-fa and FBP-fa were then placed in an oven and polymerized stepwise at 140, 160, 180, 200, 220 and 240 °C for 1 h each, therefore obtaining poly(GU-fa) and poly(FBP-fa), respectively.

3. Results and discussion

3.1. Synthesis of tri-furan functional bis-benzoxazine

The pathway adopted for obtaining polybenzoxazine was stared from the furan-functional bis-phenol (FBP) for preparation of tri-furan functional bis-benzoxazine and then by thermally activated polymerization to obtain poly(FBP-fa). FBP was readily synthesized through the condensation of guaiacol and furfural in the presence of NaOH [43]. In addition, the tri-furan functional bis-benzoxazine (FBP-fa) was obtained by the Mannich condensation of FBP, furfurylamine and paraformaldehyde via a solventless procedure as illustrated in Scheme 2. Moreover, final products with excellent purity were also achieved in this study, which is in order to eliminate the effects of impurities on the ring-opening polymerization of oxazine rings and properties of resulted thermosets [44].

The structures of FBP were characterized by FT-IR (Fig. S1), and ^{1}H and ^{13}C NMR (Fig. S2) spectroscopies. As shown in Fig. 1, the peak at 8.56 ppm is assigned to the phenolic −OH group. The characteristic proton resonances of the furan ring appear at 7.52, 6.33 and 6.08 ppm, respectively. Besides, a singlet peak at 5.72 ppm is due to the benzylic proton, and the protons originated from the methoxy exhibit a singlet at 3.78 ppm.

The chemical structures of the newly obtained benzoxazine monomer, FBP-fa, were confirmed by NMR (Figs. S3 and S4) and FT-IR spectroscopies. As also shown in Fig. 1, the furan ring is characterized by the resonances at around 7.60 ppm (−OC*H*−CH) and at 6.02–6.39 ppm (═C*H*−C*H*═). In addition, the proton resonance for the benzylic proton can be found at 5.28 ppm, and the protons attributed to the methoxy show a singlet at 3.68 ppm. The typical proton resonance assigned to the O−CH_2−N group in oxazine ring of this tri-furan functional bis-benzoxazine exhibits a singlet at 4.79 ppm. Moreover, the last two signals, which are attributed to the proton resonances for

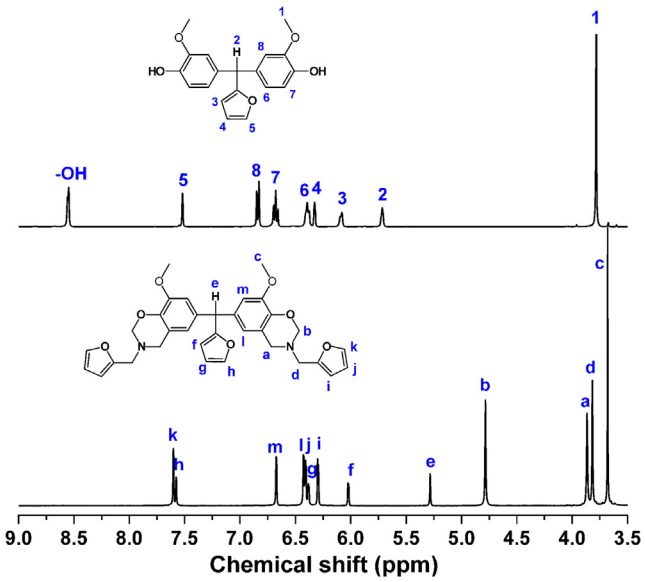

Fig. 1. ^{1}H NMR spectra of FBP and FBP-fa in DMSO-d_6.

the Ar−CH_2−N of oxazine ring and protons of RN−CH_2−fur in furfuryl group, respectively, present rather close chemical shifts. In order to assign the methylene protons from oxazine ring and furfuryl groups, 2D ^{1}H-^{1}H NOESY was then performed (Fig. S5). The useful information observed from the NOE interaction by RN−CH_2−fur with −OC*H*−CH protons from the furfuryl group is sufficient to confirm the rest assignments in ^{1}H NMR spectrum of FBP-fa as shown in Fig. 1.

^{13}C NMR spectrum was also recorded to further ascertain the structure of FBP-fa. The resonances of carbons in FBP-fa were simply assigned to protons based on the couplings observed in ^{1}H-^{13}C HMQC NMR spectra (Fig. S6). As can be observed from Fig. 2, the typical carbon resonance pair for Ar−CH_2−N− and −O−CH_2−N− appears at 49.32 and 81.74 ppm, respectively. The characteristic carbon signal for the RN−CH_2−fur in furfuryl group locates at 47.91 ppm. Besides, the carbon resonances of furan group can be observed at around 142.58 and 108.05–111.03 ppm. Moreover, the singlet peak at 49.66 ppm is assigned to the benzylic resonance, and the carbon resonance originated from the methoxy exhibits a peak at 55.87 ppm.

FT-IR spectrum was further recorded to verify the oxazine and furan rings in the tri-furan functional bis-benzoxazine monomer. As shown in Fig. 3, the existence of oxazine ring in FBP-fa is apparent by a characteristic band centered at 1227 cm^{-1}, which is attributed to the stretching vibrations of aromatic C−O linkages [45]. Besides, the characteristic benzoxazine related modes including C−O stretching mode of the oxazine ring and the mode of phenolic ring vibration are located at 922 cm^{-1} [46]. Moreover, the presence of furan ring is supported by the typical bands centered at 1496 cm^{-1} (C═C stretching), 1073 cm^{-1} (C−O antisymmetric stretching) and 734 cm^{-1} (C−H out-of-plane in-phase wagging), respectively [32]. Furthermore, the results from elemental analysis as well as high-resolution mass spectrometry give more sufficient evidence for the excellent purity of

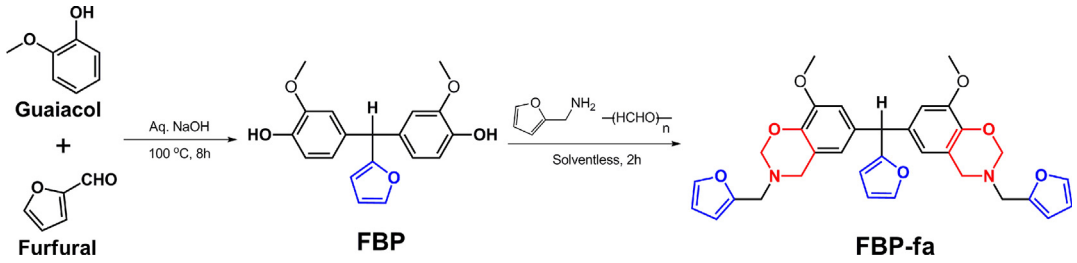

Scheme 2. Synthesis of Tri-Furan Functional Bis-Benzoxazine Monomer.

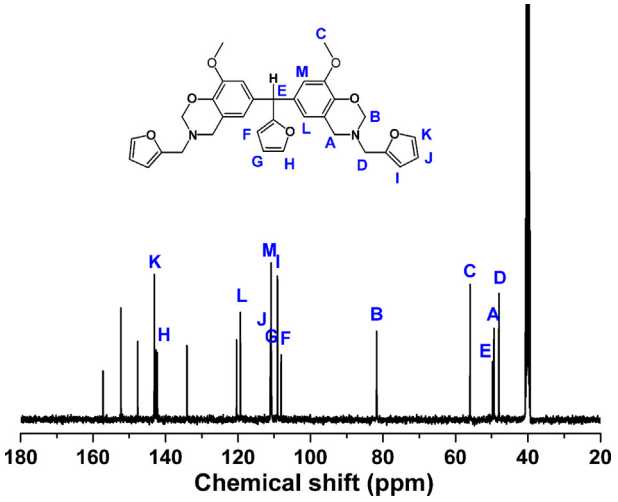

Fig. 2. ^{13}C NMR spectrum of FBP-fa in DMSO-d_6.

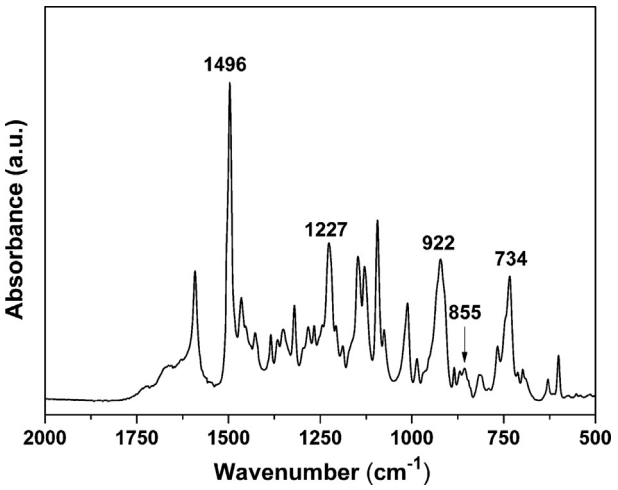

Fig. 3. FT-IR spectrum of FBP-fa.

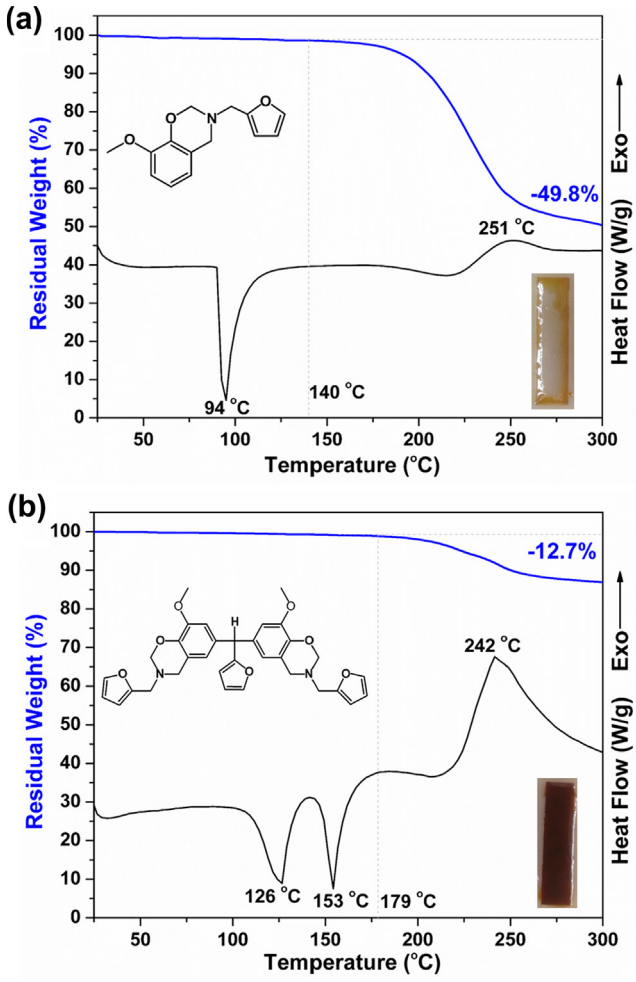

Fig. 4. (a) DSC *vs* TGA thermograms of GU-fa. The inset is a photo of resulted polybenzoxazine sample of poly(GU-fa), clearly showing that a large amount of resin was evaporated during the polymerization. (b) DSC *vs* TGA thermograms of FBP-fa. The inset is a photo of polybenzoxazine film of poly(FBP-fa).

FBP-fa obtained in this study.

3.2. Polymerization behaviors of benzoxazines

Herein, a counterpart, guaiacol and furfurylamine based monofunctional benzoxazine monomer (GU-fa) has also been synthesized (the detailed structural characterization can be found in Figs. S7–S11), which aims to achieve deep insights into the polymerization behavior of the tri-furan functional bis-benzoxazine and properties of the corresponding polybenzoxazine. In particular, GU-fa was also highly purified prior to its use, in order to avoid the impurity-related interferences.

DSC was adopted to investigate the polymerization processes of benzoxazine monomers as shown in Fig. 4. Both benzoxazines show sharp and intense melting endotherms, which further indicates their excellent purity. GU-fa shows a melting peak at 94 °C, while FBP-fa exhibits two melting peaks at 126 and 153 °C, respectively. Besides, the DSC thermograms illustrate that the polymerization process of GU-fa started at 215 °C with its maximum located at 251 °C (see Table 1). Additionally, the onset of polymerization is shifted to as low as 204 °C for FBP-fa, and the corresponding maximum for the exothermic peak is reduced to 242 °C. Moreover, the heat of polymerization of FBP-fa is 232 J/g, which is much greater than that of Gu-fa (125 J/g). Such result is quite normal since FBP-fa is a bis-benzoxazine with double of reactive groups in one molecule. Nevertheless, the heat polymerization of both guaiacol-based benzoxazine monomers are much lower than the heat of

Table 1
Results of the DSC Analysis of Benzoxazine Monomers.

Monomer	Onset temp (°C)	Max temp (°C)	Heat of polymerization (J/g)
GU-fa	215	251	125
FBP-fa	204	242	232

polymerization of other reported typical benzoxazine monomers (~300 J/g) [47]. It is likely that the cross-linking reaction of both monomers were impeded by the *ortho*-substituted methoxy group from guaiacol. The cross-linking of benzoxazine is generally taken placed through the substitution reaction between opened oxazine ring and benzene ring. Moreover, it is well know that the reactivity in benzene reduces in the order from the *ortho* to *para* to *meta* respected to the phenolic OH in polybenzoxazine [5]. However, the *ortho* positions of oxygen in oxazine ring for GU-fa and FBP-fa are all substituted by methoxy group, leading to the very low heat of polymerization of both monomers.

Comparisons of TGA and DSC thermograms for GU-fa and FBP-fa were also studied as shown in Fig. 4. The initial weight loss of GU-fa appears at 140 °C, and evaporation of an excessive amount, as high as 20% is observed before the onset of polymerization (Fig. 4a). Besides, a further ~30% of weight loss can be found in the polymerization process, which can be attributed to the cleavage of zwitterionic intermediate, forming extraordinary unstable phenolic species and N-

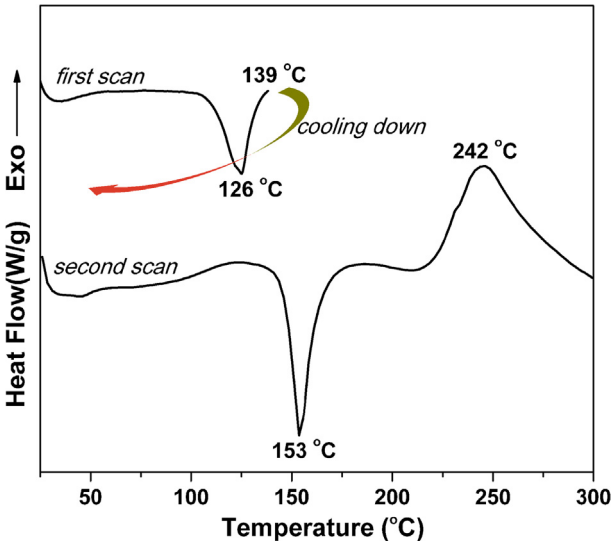

Fig. 5. DSC thermograms of FBP-fa recorded under nitrogen at a heating rate of 10 °C/min. The first DSC scan for FBP-fa was stopped at 139 °C, and after cooling to room temperature the second scan was performed to 300 °C.

methyleneaniline [48]. As a result, the film sample of poly(GU-fa) was failed to obtain by using the general casting polymerization method as seen from the inset photo in Fig. 4a. On the contrary, the initial weight loss of FBP-fa starts around 179 °C, and the evaporation has been significantly reduced to 3.5% before the onset of polymerization due to its relatively higher molecular weight. In addition, the weight loss in the polymerization process of FBP-fa is also much lower compared with that of GU-fa. Therefore, only the film sample of poly(GU-fa) can be successfully obtained as shown in Fig. 4b.

Interestingly, a phase change of crystal-to-crystal transition was observed in FBP-fa. To the best of our knowledge, such unique thermal behavior has never been found in bio-based benzoxazines. As shown in Fig. 4b, FBP-fa presents an endothermic peak at 126 °C and a very small exothermic peak at 141 °C, followed by another sharp endothermic peak at 153 °C. In addition, this phase transition disappears after the first scanning by heating to 139 °C at a heating rate of 10 °C/min under N_2 (see the DSC profiles of Fig. 5), clearly indicating that the monotropic characteristic between these two crystal forms in FBP-fa according to the Burger-Ramberger heat-of-fusion rule [49]. In addition, the maximum of the exothermic peak of FBP-fa exhibits no variations after the thermal treatment of the first scanning as shown in Fig. 5, strongly indicating that the crystal phase of this bio-based resin plays no influence on the polymerization behavior.

In situ FT-IR spectra for benzoxazines were recorded in order to qualitatively analyze their structural changes. Each spectrum was recorded after the hot cell temperature reached the desired temperature for 1 h. As can be seen in Fig. 6, the typical bands at 1234 and 1227 cm^{-1} (stretching vibrations of aromatic C—O linkages) and 933 and 922 cm^{-1} (benzoxazine related mode) can be applied to monitor the polymerization process of oxazine rings in GU-fa and FBP-fa, respectively. Both typical bands decrease during the heating, and fully disappear after the final thermal treatment at 240 °C for 1 h. Meanwhile, the broad bands in the region of 3600–3000 cm^{-1}, which can be assigned to the multiple —OH stretching modes of phenolic groups [50], gradually emerge as increasing the temperatures. Additionally, the characteristic FT-IR signals of the furan group at 732 and 734 cm^{-1} for GU-fa and FBP-fa, respectively, decease during the polymerization. Moreover, the typical bands of the furan ring at around 1590 cm^{-1} for both monomers are broadened as increasing the temperature, suggesting the formation of substituted furan rings [38]. However, the characteristic bands of furan group cannot be completely disappeared after the polymerization cycles performed in this study, clearly

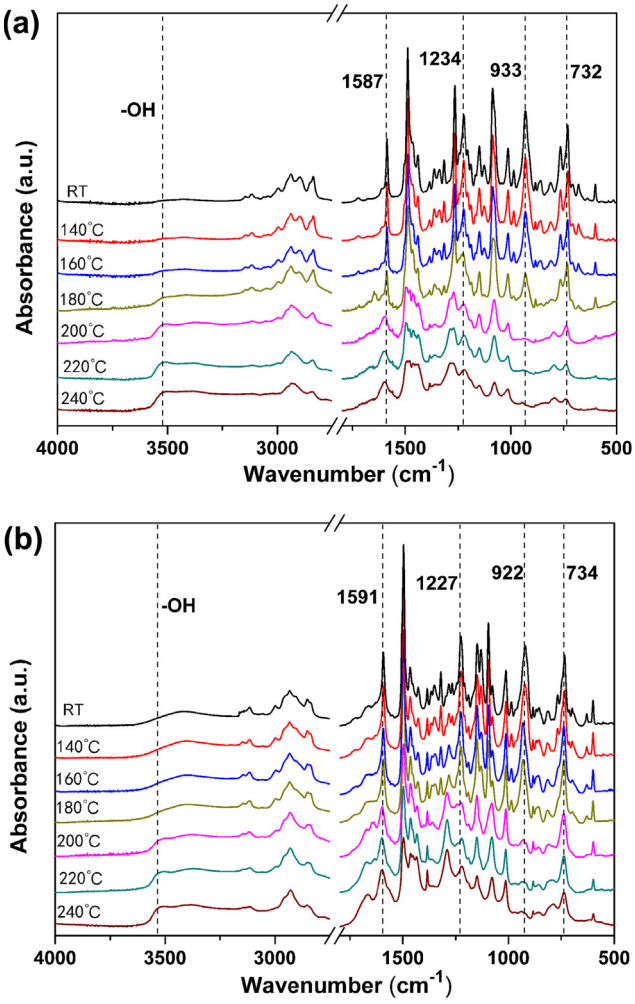

Fig. 6. (a) *In situ* FTIR spectra of GU-fa (a) and FBP-fa (b) after various thermal treatments.

indicating that the completion of the polymerization of furan group requires a much higher polymerization temperature. Herein, we did not examine the polymerization behaviors at higher temperature because obvious weight loss has been obverted from the above TGA measurements for both monomers. Therefore, on the basis of the details observed from DSC and *in situ* FT-IR analyses, we propose a simplified polymerization process of FBP-fa as depicted in Scheme 3.

3.3. Thermal properties of polybenzoxazines

TMA and DMA analyses were applied to investigate the thermomechanical properties of polybenzoxazine thermosets. As mentioned above, the film samples of poly(GU-fa) were difficult to produce since large amounts of sample evaporation during the polymerization process. Thus only the thermomechanical properties of poly(FBP-fa) were evaluated in this section. Fig. 7 shows the TMA curve of poly(FBP-fa). The coefficient of thermal expansion (CTE) of poly(FBP-fa) is found to be 40.6 ppm/°C over a temperature range of 50–250 °C. Particularly, this thermal expansion value is much lower than the CET values of previously reported epoxy resins (40–120 ppm/°C) [51]. Besides, the CTE value of poly(FBP-fa) is also lower than many other reported polybenzoxazines [52,53]. Moreover, a T_g value of 287 °C is observed for poly(FBP-fa) from the TMA curve.

The DMA curves of poly(FBP-fa) are shown in Fig. 8 for the storage modulus (*E'*), loss modulus (*E''*) and tan δ. The spectra exhibits clearly that *E'* maintains a stable value and starts decreasing in the T_g region.

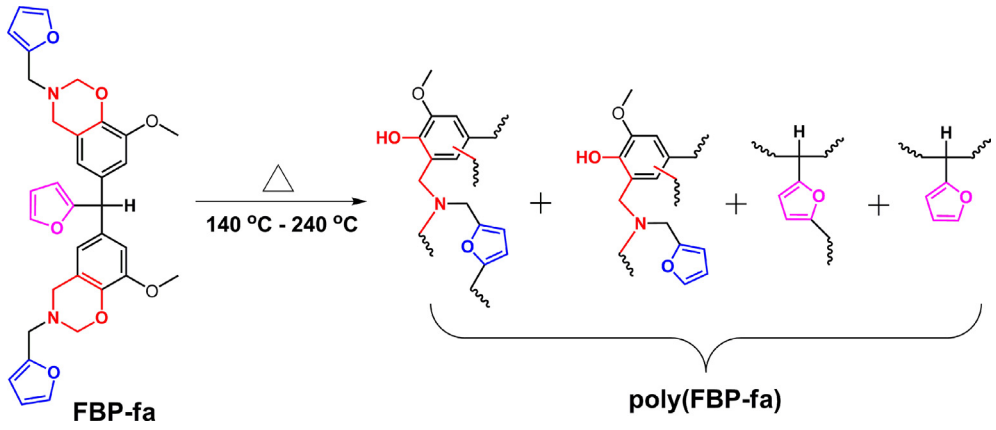

Scheme 3. Schematic Repersentation of Proposed Polymerization Process of FBP-fa.

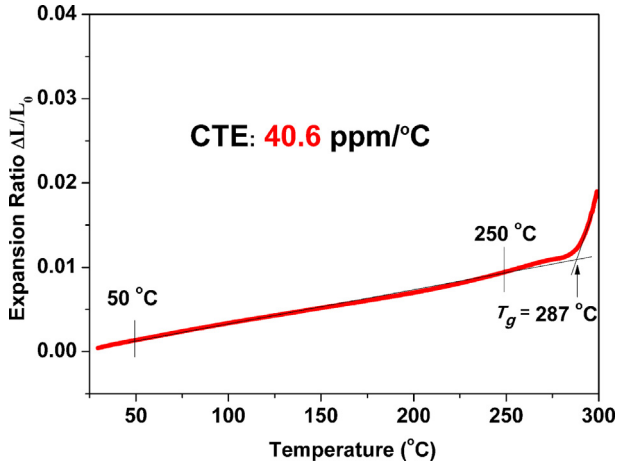

Fig. 7. Thermomechanical analysis of thermoset film of poly(FBP-fa).

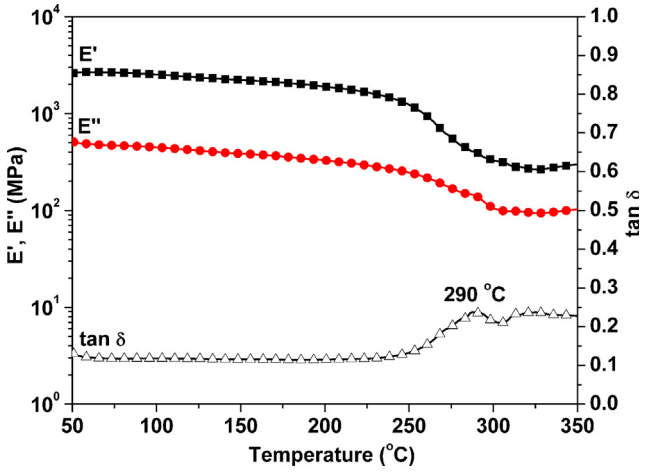

Fig. 8. Dynamic mechanical spectra of thermoset film of poly(FBP-fa).

Besides, the modulus tends to increase in the rubbery plateau as depicted in Fig. 8, indicating the existence of restriction in the segmental mobility. Such behavior is not unexpected since the additional polymerization of the residual unreacted furan groups at elevated temperature can further increase the cross-linking density of polybenzoxazine. As also shown in the figure, the T_g determined from tan δ is as high as 290 °C. This result is in good agreement with that measured by above TMA. Another resolved relaxation at around 320 °C has also been found from the tan δ peak, implying the further polymerization of

Table 2
Thermal Properties of Resveratrol-based Polybenzoxazines.

Sample	T_g (TMA) (°C)	T_g (DMA) (°C)	CTE[a] (ppm/°C)
poly(FBP-fa)	287	290	40.6

[a] Coefficient of thermal expansion is recorded from 50 to 250 °C.

residual furan groups at elevated temperatures and formation of cross-linked networks with much higher cross-lining density. In addition, poly(FBP-fa) shows a much higher T_g temperature than poly(GU-fa), which was reported as low as 148 °C [29]. The polybenzoxazine derived from GU-fa shows poor performance is mainly attributed to its low cross-linking density. Many polybenzoxazines derived from mono-functional benzoxazines show small linear or branched oligomers due to the competing terminating effect of intramolecular hydrogen bonding of the active species. As are result, only a few exceptional mono-functional benzoxazines can polymerize to from cross-linked networks. The data of thermomechanical properties from both TMA and DMA for poly(FBP-fa) are summarized in Table 2.

TGA was then performed to study the thermal stability of polybenzoxazines derived from GU-fa and FBP-fa as shown in Fig. 9. The thermal stability of both bio-based polybenzoxazines, T_{d5} and T_{d10}, defined as temperatures at which a weight-loss of 5% and 10%, respectively, and char yield (Yc), defined as the residual char yield value at 800 °C in nitrogen, are all summarized in Table 3.

In general, the initial decomposition temperatures of thermosets derived from mono-oxazine benzoxazines are lower than ones based on bis- or main-chain type benzoxazine resins [52]. The initial

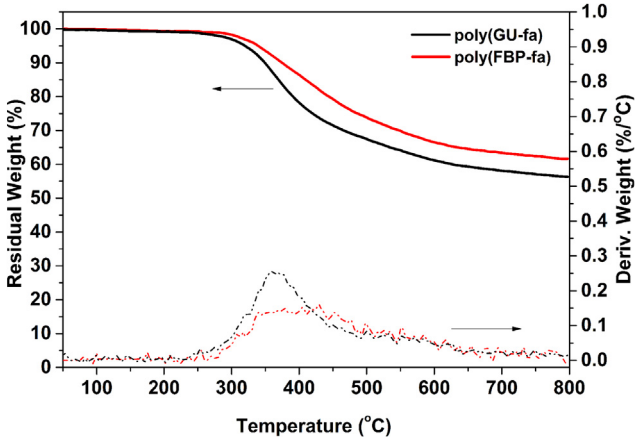

Fig. 9. Thermogravimetric analysis of poly(GU-fa) and poly(FBP-fa) in nitrogen.

Table 3
Thermal Stability and Heat Release Properties of poly(GU-fa) and poly(FBP-fa).

Sample	T_{d5} (°C)	T_{d10} (°C)	Yc (wt.%)	HRC (J g^{-1} K^{-1})	THR (KJ g^{-1})
poly(GU-fa)	320	348	56	70.6	6.5
poly(FBP-fa)	340	375	62	30.4	5.8

decomposition of mono-oxazine functional benzoxazines derived polybenzoxazines are mostly taken place from secondary amides and the terminal Schiff base as structural defects [38]. As expected, the degradation temperatures of poly(FBP-fa) reflected on the T_{d5} and T_{d10} are 340 and 375 °C, respectively, which are significantly higher than poly(GU-fa). Besides, poly(FBP-fa) shows a Yc value of 62% at 800 °C in nitrogen atmosphere, which is also much higher than that of poly(GU-fa) (56%). The incorporation of the three furan groups as part of the very same bis-benzoxazine greatly improve the thermal stability of its corresponding polybenzoxazine when compared with other traditional bis-benzoxazine resins [5]. As mentioned above, the further cross-linking process from residual furan groups in poly(FBP-fa) at elevated temperatures can effectively decrease the fractions from terminal defects.

The broadening of the DTG peaks in Fig. 9 indicates a very slow rate of decomposition over a wide temperature range. Some recent reports have indicated that the thermosets derived from furan-containing benzoxazines generally performed good anti-flame characteristics [32,34,39]. The flammability of poly(GU-fa) and poly(FBP-fa) was evaluated by the limiting oxygen index (LOI), which can be calculated by van Krevelen equation based on the Yc values from TGA measurement [54]. As a result, poly(GU-fa) and poly(FBP-fa) show LOI values of 39.9 and 42.3, respectively. Both polybenzoxazines have high LOI values in the self-extinguishing region (LOI > 28) [55]. Microscale combustion calorimetry (MCC) analysis was also performed to further evaluate the performance of flammability of poly(GU-fa) and poly(FBP-fa). As shown in Fig. 10, MCC characterization of poly(GU-fa) and poly (FBP-fa) exhibit heat release capacity (HRC) values of 79.6 and 30.4 J g^{-1} K^{-1}, respectively. In addition, poly(GU-fa) reveals THR values of 6.5 KJ g^{-1}, while poly(FBP-fa) exhibits a relatively lower total heat release (THR) value of 5.8 KJ g^{-1} (Fig. 11). Herein, the data of fire-related properties of both thermosets are also summarized in Table 3. Surprisingly, the HRC value of poly(FBP-fa) obtained in this study is much lower than the previously reported 47 polymers [56]. Moreover, poly(FBP-fa) also shows much lower flammability than many other reported polybenzoxazines [27,39,52]. It has been well-known that the

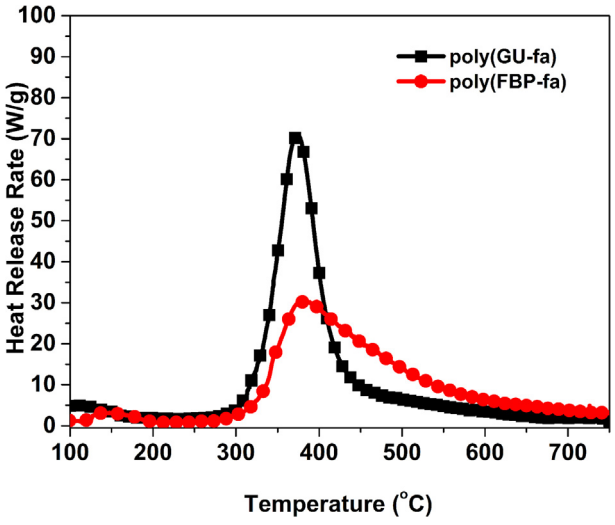

Fig. 10. Heat release rate (HRR) *vs* temperature for poly(GU-fa) and poly(FBP-fa).

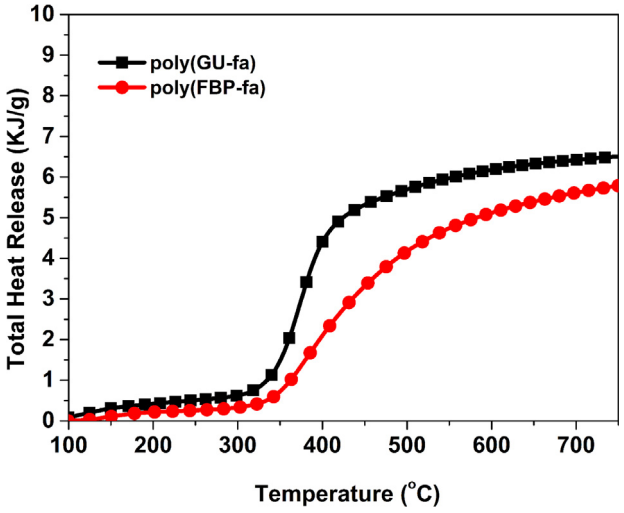

Fig. 11. Total heat release (THR) *vs* temperature for poly(GU-fa) and poly(FBP-fa).

HRC less than 300 J/g·K can be regarded as self-extinguishing whereas materials with values less than 100 J/g·K are considered non-ignitable [57]. Consequently, the highly cross-linked networks generated from this newly developed tri-furan functional bis-benzoxazine results in a substantial reduction of HRC values. Therefore, the newly obtained bio-based benzoxazine resin derived from renewable guaiacol, furfural and furfurylamine opens new opportunities for the application as matrix of high-performance composites.

4. Conclusion

A new tri-furan functional bis-benzoxazine resin, FBP-fa, was successfully synthesized using guaiacol, furfural, furfurylamine, and paraformaldehyde as staring materials. The chemical structures of FBP-fa were characterized by NMR and FT-IR spectroscopies and elemental analysis. Additionally, the resulting polybenzoxazine obtained, poly (FBP-fa), showed a high T_g of 290 °C, T_{d5} and T_{d10} of 340 °C and 375 °C, respectively, and a high char yield value of 62%, indicating its excellent thermal stability. Notably, poly(FBP-fa) also exhibited to be a flame retardant material possessed the low HRC of 30.4 J g^{-1} K^{-1} as well as THR value of 5.8 KJ g^{-1}. These results have highly impacts on designing of high-performance polybenzoxazine thermosets based on fully bio-based benzoxazine resins.

CRediT authorship contribution statement

Rui Yang: Investigation, Data curation, Writing - original draft. **Mengchao Han:** Investigation, Data curation, Investigation, Data curation. **Boran Hao:** Data curation, Writing - original draft. **Kan Zhang:** Conceptualization, Supervision, Writing - review & editing.

Declaration of Competing Interest

The authors declare that they have no known competing financial interests or personal relationships that could have appeared to influence the work reported in this paper.

Acknowledgements

This worked was funded by the National Natural Science Foundation of China (51603093), the Natural Science Foundation of Jiangsu Province (BK 20160515), and China Postdoctoral Science Foundation (2018T110451).

Appendix A. Supplementary material

Supplementary data to this article can be found online at https://doi.org/10.1016/j.eurpolymj.2020.109706.

References

[1] H. Ishida, P. Froimowicz, Advanced and Emerging Polybenzoxazine Science and Technology, Elsevier, Amsterdam, 2017.
[2] S. Alper-Hayta, E. Aki-Sener, B. Tekiner-Gulbas, I. Yildiz, O. Temiz-Arpaci, I. Yalcin, N. Altanlar, Synthesis, antimicrobial activity and QSARs of new benzoxazine-3-ones, Eur. J. Med. Chem. 41 (2006) 1398–1404.
[3] S. Vaithilingam, K.P. Jayanthi, A. Muthukaruppan, Synthesis and characterization of cardanol based fluorescent composite for optoelectronic and antimicrobial applications, Polymer 108 (2017) 449–461.
[4] N. Gupta, S. Sharma, A. Raina, N.A. Dangroo, S. Bhushan, P.L. Sangwan, Synthesis and anti-proliferative evaluation of novel 3,4-dihydro-2H-1,3-oxazine derivatives of bakuchiol, RSC Adv. 6 (2016) 106150–106159.
[5] H. Ishida, T. Agag, Handbook of Benzoxazine Resins, Elsevier, Amsterdam, 2011.
[6] N.N. Ghosh, B. Kiskan, Y. Yagci, Polybenzoxazines-new high performance thermosetting resins: synthesis and properties, Prog. Polym. Sci. 32 (2007) 1344–1391.
[7] L. Han, M.L. Salum, K. Zhang, P. Froimowicz, H. Ishida, Intrinsic self-initiating thermal ring-opening polymerization of 1, 3-benzoxazines without the influence of impurities using very high purity crystals, J. Polym. Sci., Part A: Polym. Chem. 55 (2017) 3434–3445.
[8] K. Zhang, X. Yu, Catalyst-free and low-temperature terpolymerization in a single-component benzoxazine resin containing both norbornene and acetylene functionalities, Macromolecules 51 (2018) 6524–6533.
[9] Y.T. Liao, Y.C. Lin, S.W. Kuo, Highly thermally stable, transparent, and flexible polybenzoxazine nanocomposites by combination of double-decker-shaped polyhedral silsesquioxanes and polydimethylsiloxane, Macromolecules 50 (2017) 5739–5747.
[10] A.F.M. El-Mahdy, S.W. Kuo, Direct synthesis of poly(benzoxazine imide) from an ortho-benzoxazine: its thermal conversion to highly cross-linked polybenzoxazole and blending with poly(4-vinylphenol), Polym. Chem. 9 (2018) 1815–1826.
[11] K. Zhang, J. Liu, S. Ohashi, X. Liu, Z. Han, H. Ishida, Synthesis of high thermal stability polybenzoxazoles via ortho-imide-functional benzoxazine monomers, J. Polym. Sci. Part A: Polym. Chem. 53 (2015) 1330–1338.
[12] Q.C. Ran, D.X. Zhang, R.Q. Zhu, Y. Gu, The structural transformation during polymerization of benzoxazine/FeCl3 and the effect on the thermal stability, Polymer 53 (2012) 4119–4127.
[13] C.H. Chen, C.H. Lin, J.M. Hon, M.W. Wang, T.Y. Juang, First halogen and phosphorus-free, flame-retardant benzoxazine thermosets derived from main-chain type bishydroxydeoxybenzoin-based benzoxazine polymers, Polymer 154 (2018) 35–41.
[14] K. Zhang, L. Han, P. Froimowicz, H. Ishida, A smart latent catalyst containing o-trifluoroacetamide functional benzoxazine: precursor for low temperature formation of very high Performance polybenzoxazole with low dielectric constant and high thermal stability, Macromolecules 50 (2017) 6552–6560.
[15] J. Wu, Y. Xi, G.T. Mccandless, Y. Xie, R. Menon, Y. Patel, R. Menon, Y. Patel, D.J. Yang, S.T. Iacono, B.M. Novak, Synthesis and characterization of partially fluorinated polybenzoxazine resins utilizing octafluorocyclopentene as a versatile building block, Macromolecules 48 (2015) 6087–6095.
[16] K. Zhang, X. Yu, S.W. Kuo, Outstanding dielectric and thermal properties of main chain-type poly(benzoxazine-co-imide-co-siloxane)-based cross-linked networks, Polym. Chem. 10 (2019) 2387–2396.
[17] K.C. Chen, H.T. Li, S.C. Huang, W.B. Chen, K.W. Sun, F.C. Chang, Synthesis and performance enhancement of novel novel polybenzoxazine with low surface free energy, Polym. Int. 60 (2011) 1089–1096.
[18] W.C. Chen, S.W. Kuo, Ortho-imide and ally groups effects on highly thermally stable polybenzoxazine/double-decker-shape polyhedral silsesquioxane hybrids, Macromolecules 51 (2018) 9602–9612.
[19] C.J. Moore, Synthetic polymers in the marine environment: A rapidly increasing, long-term threat, Environ Res. 108 (2008) 131–139.
[20] R. Auvergne, S. Caillol, G. David, B. Boutevin, Biobased thermosetting epoxy: present and future, Chem. Rev. 114 (2014) 1082–1115.
[21] Y. Liu, L. Cao, J. Luo, Y. Peng, Q. Ji, J. Dai, J. Zhu, X. Liu, Biobased nitrogen- and oxygen-codoped carbon materials for high-performance supercapacitor, ACS Sustain. Chem. Eng. 7 (2018) 2763–2773.
[22] Y. Dai, N. Teng, X. Shen, Y. Liu, L. Cao, J. Zhu, X. Liu, Syntheis of biobased benzoxazines suitable for vacuum-assisted resin transfer molding process via introduction of soft silicon segment, Ind. Eng. Chem. Res. 57 (2018) 3091–3102.
[23] A. Gandini, Polymers from Renewable Resources: A challenge for the future of macromolecular material, Macromolecules 41 (2008) 9491–9504.
[24] A. Gandini, Furans as offspring of sugars and polysaccharides and progenitors of a family of remarkable polymers: A review of recent progress, Polym. Chem. 1 (2010) 245–251.
[25] P.T. Anastas, J.C. Warner, Handbook of Green Chem, Theory and Practice, Oxford University Press, New York, 1998.
[26] E. Calý, A. Maffezzoli, G. Mele, F. Martina, S.E. Mazzetto, A. Tarzia, C. Stifani, Synthesis of a novel cardanol-based benzoxazine monomer and environmentally sustainable production of polymers and bio-composites, Green Chem. 9 (2007) 754–759.
[27] K. Zhang, M. Han, Y. Liu, P. Formowicz, Design and synthesis of bio-based high performance tri-oxazine benzoxazine resin via natural renewable resources, ACS Sustainable Chem. Eng. 7 (2019) 9399–9407.
[28] P. Thirukumaran, A.S. Parveen, M. Sarojadevi, Synthesis and copolymerization of fully biobased benzoxazines from renewable resources, ACS Sustain. Chem. Eng. 2 (2014) 2790–2801.
[29] C.F. Wang, J.Q. Sun, X.D. Liu, A. Sudo, T. Endo, Synthesis and copolymerization of fully bio-based benzoxazines from guaiacol, furfurylamine and stearylamine, Green Chem. 14 (2012) 2799–2806.
[30] N. Teng, S. Yang, J. Dai, S. Wang, J. Zhao, J. Zhu, X. Liu, Making benzoxazine greener and stronger: Renewable resource, microwave irradiation, green solvent, and excellent thermal properties, ACS Sustain. Chem. Eng. 7 (2019) 8715–8723.
[31] B. Kiskan, Y. Yagci, Thermally curable benzoxazine monomer with a photodimerizable coumarin group, J. Polym. Sci., Part A: Polym. Chem. 45 (2007) 1670–1676.
[32] P. Froimowicz, C.R. Arza, L. Han, H. Ishida, Smart, sustainable, and ecofriendly chemical design of fully bio-based thermally stable thermosets based on benzoxazine chemistry, ChemSusChem 9 (2016) 1921–1928.
[33] Y. Peng, J. Dai, Y. Liu, L. Cao, J. Zhu, X. Liu, Bio-based polybenzoxazine modified melamine sponges for selective absorption of organic solvent in water, Adv. Sustain. Sys. 3 (2019) 1800126.
[34] J. Dai, N. Teng, Y. Peng, Y. Liu, L. Gao, J. Zhu, X. Liu, Biobased benzoxazine derived from daidzein and furfurylamine: Microwave-assisted synthesis and thermal properties investigation, ChemSusChem 11 (2018) 3175–3183.
[35] X. Shen, J. Dai, Y. Liu, X. Liu, J. Zhu, Synthesis of high performance polybenzoxazine networks from bio-based furfurylamine: Furan vs benzene ring, Polymer 122 (2017) 258–269.
[36] X. Liu, R. Zhang, T. Li, P. Zhu, Q. Zhuang, Novel fully biobased benzoxazines from rosin: Synthesis and properties, ACS Sustain. Chem. Eng. 5 (2017) 10682–10692.
[37] S.P. Teong, G. Yi, Y. Zhang, Hydroxymethylfurfural production from bioresources: past, present and future, Green Chem. 16 (2014) 2015–2026.
[38] Y.L. Liu, C.I. Chou, High performance benzoxazine monomers and polymers containing furan groups, J. Polym. Sci., Part A: Polym. Chem. 43 (2005) 5267–5282.
[39] K. Zhang, Y. Liu, H. Ishida, Polymerization of a smart AB-type benzoxazine monomer toward different polybenzoxazine networks: When Diels-Alder reaction meets benzoxazine chemistry in a single component resin, Macromolecules 52 (2019) 7386–7395.
[40] I. Hamerton, S. Thompson, B.J. Howlin, New method to predict the thermal degradation behavior of polybenzoxazines from empirical data using structure property relationships, Macromolecules 46 (2013) 7605–7615.
[41] T. Periyasamy, K.P. Asrafali, S. Muthusamy, S.C. Kim, Replacing bisphenol-A with bisguaiachol-F to synthesize polybenzoxazines for a pollution-free environment, New J. Chem. 40 (2016) 9313–9319.
[42] R.E. Lyon, N. Safronava, J.G. Quintiere, S.I. Stoliarov, R.N. Walters, S. Crowley, Materials properties and fir test results, Fire. Mater. 38 (2014) 264–278.
[43] S.S. Nagane, S.S. Kuhire, S.R. Mane, P.P. Wadgaonkar, Partially bio-based aromatic poly (ether sulfone) s bearing pendant furyl groups: synthesis, characterization and thermo-reversible cross-linking with a bismaleimide, Polym. Chem. 10 (2019) 1089–1098.
[44] S. Ohashi, D. Iguchi, T.R. Heyl, P. Froimowicz, H. Ishida, Quantitative studies on the p-substituent effect of the phenolic component on the polymerization of benzoxazines, Polym Chem. 9 (2018) 4194–4204.
[45] J. Dunkers, H. Ishida, Vibrational assignments of 3-alkyl-3, 4-dihydro-6-methyl-2H-1,3-benzoxazines in the Fingerprint Region, Spectrochim. Acta. 51 (1995) 1061–1074.
[46] L. Han, D. Iguchi, P. Gil, T.R. Heyl, V.M. Sedwick, C.R. Arza, S. Ohashi, D.J. Lacks, H. Ishida, Oxazine ring-related vibrational modes of benzoxazine monomers using fully aromatically substituted, deuterated, 15N isotope exchanged, and oxazine-ring-substituted compounds and theoretical calculations, J. Phys. Chem. A. 121 (2017) 6269–6282.
[47] K. Zhang, M. Han, L. Han, H. Ishida, Resveratrol-based tri-functional benzoxazines: Synthesis, characterization, polymerization, and thermal and flame retardant properties, Eur. Polym. J. 116 (2019) 526–533.
[48] N.K. Sini, T. Endo, Toward elucidating the role of number of oxazine rings and intermediates in the benzoxazine backbone on their thermal characteristics, Macromolecules 49 (2016) 8466–8478.
[49] A. Burger, R. Ramberger, On the polymerization of pharmaceuticals and other molecular ctrystals, Microchim. Acta 2 (1979) 259–271.
[50] H.D. Kim, H. Ishida, A study on hydrogen bonding in controlled-structure benzoxazine model oligomers, Macromol. Symp. 195 (2003) 123–140.
[51] J.A. Dudek, J.A. Kargol, Linear thermal expansion coefficients for an epoxy/glass matte-insulated solid cast transformer, Intern. J. Thermophys. 9 (1988) 245–253.
[52] K. Zhang, X. Tan, Y. Wang, H. Ishida, Unique self-catalyzed cationic ring-opening polymerization of a high performance deoxybenzoin-based 1,3-benzoxazine monomer, Polymer 168 (2019) 8–15.
[53] H.C. Chang, C.H. Lin, H.T. Lin, S.A. Dai, Deprotection-free preparation of propargyl ether-containing phosphinated benzoxazine and structure-property relationship of the resulting thermosets, J. Polym. Sci., Part A: Polym. Chem. 50 (2011) 1008–1017.
[54] D.W. Van Krevelen, Some basic aspects of flame resistance of polymeric materials, Polymer 16 (1975) 615–620.
[55] S. Mallakpour, V. Behranvand, The influence of acid-treated multi-walled carbon nanotubes on the surface morphology and thermal properties of alanine-based poly (amide-imide)/MWCNT nanocomposites system, Colloid Polym. Sci. 293 (2015) 333–339.
[56] R. E. Lyon, M. L. Janssens, Polymer Flammability, U.S. Department of Transportation, Federal Aviation Administration, Report #DOT/FAA/AR-05/14.
[57] R.N. Walters, R.E. Lyon, Molar group contributions to polymer flammability, J. Appl. Polym. Sci. 87 (2003) 548–563.